



UPPSALA
UNIVERSITET

UPTEC F 20040

Examensarbete 30 hp
Juli 2020

Investigation of Internal Diesel Injector Deposits on fuel injector performance for proposal of injector test rig test method.

David Bergstrand



UPPSALA
UNIVERSITET

**Teknisk- naturvetenskaplig fakultet
UTH-enheten**

Besöksadress:
Ångströmlaboratoriet
Lägerhyddsvägen 1
Hus 4, Plan 0

Postadress:
Box 536
751 21 Uppsala

Telefon:
018 – 471 30 03

Telefax:
018 – 471 30 00

Hemsida:
<http://www.teknat.uu.se/student>

Abstract

Investigation of Internal Diesel Injector Deposits on fuel injector performance for proposal of injector test rig test method.

David Bergstrand

With increasing demands for lowering emissions from diesel engines, bio fuel has been introduced to the fuel mixture. This fuel is based on vegetable oil with a much smaller carbon footprint than fossil fuel. The chemical composition of bio fuel has lead to deposits forming inside the fuel injector in diesel engines, these deposits are usually denoted as Internal Diesel Injector Deposits (IDID). At Scania CV AB an injector test rig is designed with the goal of creating and investigating IDID. This project has made a theoretical investigation of how IDID are formed and how this affects the mechanics inside the injector. It has also analysed injector components from a worst case scenario perspective in order to find a testing method for creating IDID in the test rig. By analysing performance changes from a build-up perspective, where IDID decreases the tolerances inside the injector, as well as friction, formed when deposits cause injector mechanics to stick together, it has been found that injector performance does hardly change from build-up and that performance changes only occur when friction is introduced. From the injector component analysis it is found that the limiting factors in rig testing come from fuel system components rather than the injector itself. This is the base for a rig running test method presented.

Handledare: Henrik Hittig & Mayte Pach
Ämnesgranskare: Per Norrlund
Examinator: Tomas Nyberg
ISSN: 1401-5757, UPTec F 20040
Tryckt av: Uppsala

Populärvetenskaplig sammanfattning

Med ett globalt mål om att minska utsläpp av växthusgaser har bio-diesel introducerats i viss procentuell mängd världen över. Bio-diesel är baserat på vegetabiliska oljor med ett mycket koldioxidutsläpp jämfört med fossil diesel.

Parallellt med förändringar av dieselns bränsleblandning jobbar motortillverkare ständigt med att förbättra och effektivisera sina motorer. Detta har lett till att moderna motorer jobbar med toleranser på mikrometer nivå och med tider på millisekunder.

Den här utvecklingen har lett till att avlagringar har upptäckts inne i injektorn, en av de mest finmekaniska komponenterna i en motor, som kan försämra motorns prestanda och i värsta fall göra att motorn inte går att starta. Dessa avlagringar kallas ofta för Internal Diesel Injector Deposits (IDID) och består främst av metalltvålar och polyamider.

På Scania CV AB byggs en testrigg för att testa injektorer för de här avlagringarna i en kontrollerad miljö. Med målet att bättre förstå varför de finns och i slutändan utveckla injektorer som är opåverkade av IDID.

Det här projektet gör en teoretisk analys av vad det är som händer när avlagringarna skapas och hur det påverkar prestandan. Den tittar också på injektorn begränsningar i syfte att hitta en testmetod för hur testriggen ska köras.

Projektet tittar på kraftförändringarna både från när IDID byggs upp i injektorn, vilket minskar toleranserna i den, och när avlagringarna är såpass tjocka att friktion introduceras till systemet. Det visar sig att krafterna från när IDID byggs upp är mycket små och deras påverkan på injektorprestanda är minimala. Att se dessa krafter i ett riggtest får ses som närmast omöjligt.

Vad som kommer att kunna ses i ett riggtest är friktion, vilket främst visar sig genom att det tar längre tid för injektorn att öppna och stänga. Vilket påverkar både tryck och flöde som kan mätas i riggen.

Utifrån detta har en testmetod skapats för körning av testriggen som går ut på att skapa IDID snabbt, tillförlitligt och mätbart medan riggen går. Från litteraturstudier verkar det vara första gången någon försöker hitta tecken på IDID medan en rigg körs.

Begränsningarna i testtriggen verkar främst ligga i andra komponenter i injektorn och testmetoden presenterar sätt att hantera detta.

Acknowledgements

First of all I want to thank my supervisors at Scania, Mayte Pach and Henrik Hittig for all the knowledge, contacts and support during the entire project. I also want to thank my subject reader at Uppsala University, Per Norrlund for checking my errors, improving my report and for the support. The team at Scania and Cummins deserve to be well recognised as they always had time to teach, discuss and listen to my ideas and reasoning. Mentioning individuals would mean this section would go on for quite a while, but if you work at Scania or Cummins and you are reading this I can guarantee you are one of them.

For more personal acknowledgments I want to thank my friends who always manages to be there and to take my mind off of things. A special thank you to Jesper Alvelid, Johan Nilsson and Ida Salmiranta.

A special not thank you to the Corona virus which is making everything less fun.

My family has always worried about me indulging in this project and to say that it is now finished will be a huge relief for them, but probably even more so for me. So thanks for your interest and for all your support.

Last but not least, thank you Fanny Holmquist for somehow finding it enjoyable to live with me even when I am loudly discussing ideas with myself in the middle of the night. All my love to you!

Also if you are reading this. Thank you I hope you enjoy it, sorry for spoiling the ending in the abstract.

Table of Contents

Abstract	II
Populärvetenskaplig sammanfattning	III
Acknowledgements	IV
List of Acronyms	VII
1 Introduction	1
1.1 Background	1
1.2 Fuel system	2
1.3 Fuel injectors	3
1.4 Internal Diesel Injector Deposits	4
1.5 Testing	5
1.5.1 Online testing	5
1.5.2 Post test analysis	6
2 Literature Review	7
2.1 Pressure drop	7
2.2 Temperature	7
2.3 Formation of IDID	8
2.4 Test fuel	9
3 Theory	10
3.1 Diesel properties	10
3.2 Fuel flow	11
3.2.1 Laminar flow	11
3.2.2 Turbulent flow	12
3.2.3 Compressible flow	13
3.3 Shear force	14
3.4 Friction	18
3.5 Drag force	18
3.6 Joukowsky pressure	19
3.7 Needle dynamics	20
4 Methodology	23
4.1 Screen test	23

4.2	Test rig	24
5	Results	26
5.1	Screen test	26
6	Discussion & Analysis	30
6.1	Screen test	30
6.2	Needle dynamics	30
6.3	Rig running method	31
7	Conclusion	33
7.1	Conclusion and Future work	33
7.2	Future work	33
	Literature	35
	Appendices	38

List of Acronyms

AIC	Adaptive Injector Characterization
B10	10% Bio-Diesel
ECU	Electronic Control Unit
EOI	End Of Injection
FAME	Fatty Acids Methyl Esters
FTIR	Fourier-Transform Infrared Spectroscopy
GCMS	Gas Chromatography-Mass Spectrometry
HVO	Hydrotreated Vegetal Oil
IDID	Internal Diesel Injector Deposits
IID	Internal Injector Deposits
SEM	Scanning Electron Microscopy
SOI	Start Of Injection
XPI	Xtra-high Pressure Injection

1 Introduction

1.1 Background

With a global strive to lower emissions and dependency on oil, modern diesel engines are now more efficient than ever before. These engines are highly complex machinery with small tolerances and highly optimised for converting the chemical energy in diesel into mechanical energy to drive a vehicle.

One of the parts that has undergone a huge change since the invention of the diesel engine is the fuel injector, what started as a mechanical pump with fixed parameters [1] has now become a fine tuned, high pressure fuel injector that sprays a precise amount of diesel direct into the cylinder.

With continuous measurements and computerised opening and closing times of the injector the fuel can be fine tuned for every fuel cycle. Modern fuel injectors work with a common-rail fuel injection which in general pumps fuel into the cylinder with pressures in excess of 200 MPa. Such high pressures create an environment of high temperature and high shear force inside the injector and with the increasing amounts of bio-fuels in diesel this has been found to create a deposit called Internal Diesel Injector Deposits (IDID) or sometimes Internal Injector Deposits (IID), however in this report IDID will be used.

IDID are sticky particles that have been found to cause changes in engine performance and also, in some cases, engines failing to start. Other studies such as Ullman et al. [2] and [3] Schwab et al. have studied the chemical composition and properties of these particles whereas other such as Goede et al. [4] and Fortunato et al. [5] have tested different aspects of deposit formation and its physical consequences.

At Scania CV AB an injector test rig has been designed and finding a test protocol to produce IDID at a short time scale would help future development of IDID resistant injector systems.

1.2 Fuel system

In fig 1.1 the fuel path to the engine is shown. From a low pressure pump fuel is taken from the fuel tank, through filters, in blue, to a high pressure pump, in teal. The pump raises the pressure and temperature of the fuel to the common rail fuel pressure, which is 200 MPa. From the high pressure pump the fuel is fed to an accumulator which is the same as a common rail. This common rail regulates the pressure and contains sensors to control the pressure output from the high pressure pump.

If the pressure is too high a release valve, in grey, at the end of the common rail is opened and lets fuel return to the high pressure pump, following the green pipe.

The fuel continues from the accumulator through the yellow high pressure pipes to the injector. From the injector the fuel is injected to the cylinder where it is mixed with air and under high compression combustion occurs transforming chemical energy in the fuel to mechanical energy and heat. The mechanical energy is what drives the engine and all of its components.

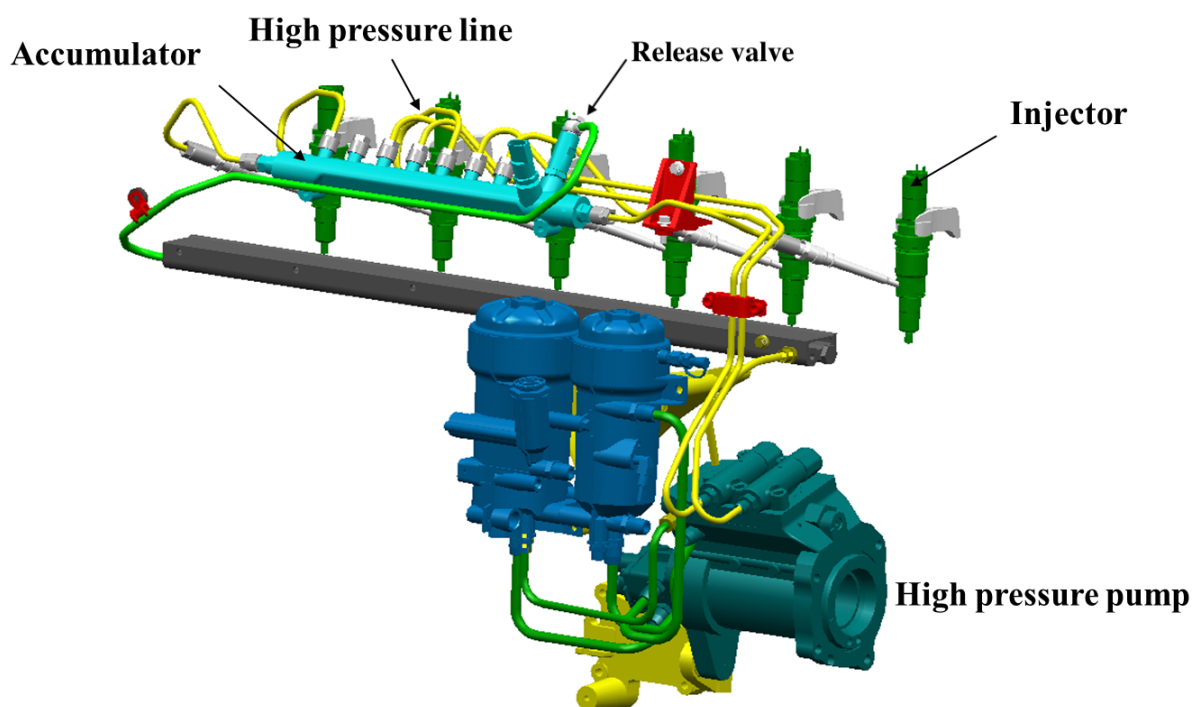


Figure 1.1: Scania/Cummins XPI fueling system. Courtesy of Cummins.

1.3 Fuel injectors

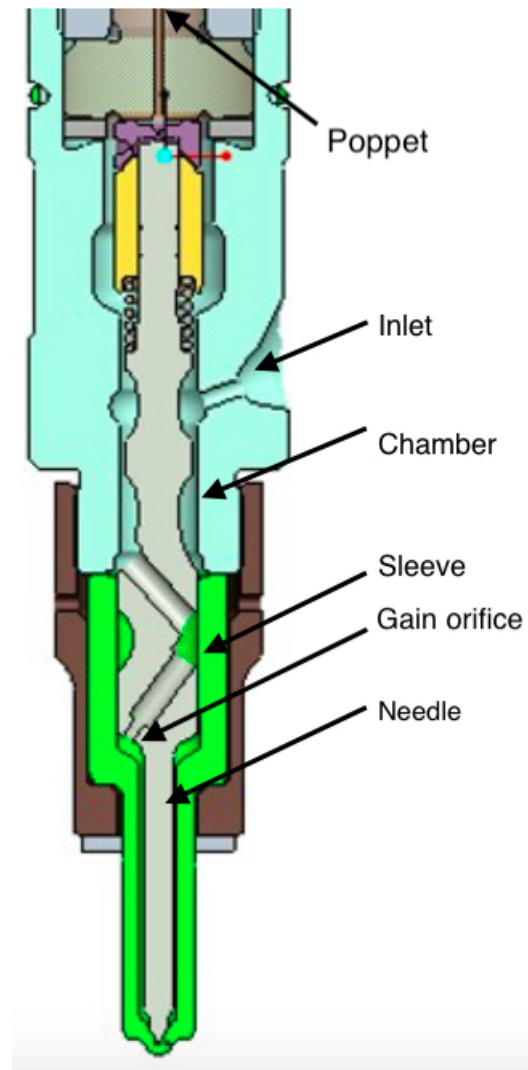


Figure 1.2: Cross section of a Scania/Cummins XPI fuel injector. Sleeve in green and needle in grey. Courtesy of Cummins.

A modern fuel injector, such as the Scania/Cummins Xtra-high Pressure Injection (XPI), which can be seen in fig 1.2, is a very delicate part of the engine. Pressurised fuel arrives from the common rail via the inlet, a channel in light blue colour in the figure. The fuel fills the sleeve, in green, and chamber, light blue, pressurising the entire injector. To open the injector a current is sent through an electromagnet lifting a poppet which opens a chamber with a lower pressure resulting in a net force to lift the needle, in grey.

When the needle is lifted the fuel can flow to the nozzle orifice which is designed to atomise the flow sending a fine and precise spray in to the cylinder. This operation is highly sophisticated where timings are in milliseconds and tolerances in micrometres, meaning if something influences the performance this can have a large impact on the

injection. The needle on the upper part of the sleeve, where the needle is widest is a gain orifice, which is designed to cause a pressure difference between the upper and the lower part of the needle, regulating the dynamics of the needle as well as functioning as a bearing for low friction. It is also there to steer the needle, which means that the tolerances here are very small. However the orifice does not restrict rotation and because of vibrations, flow and imbalances in the system the needle has been observed to rotate when it is not fully closed.

One needle design is to use a flat gain orifice seen in fig 1.3 where a flat area controls the flow and pressure difference. The length of this flat area can be found by using the angle α and the radius of the circular part of the orifice.

From field testing it has been seen that deposits attach to this area as well as the lower part of the needle, but since the tolerances are smaller at the gain orifice than the lower part it is likely that the problems caused by IDID attaching to the gain orifice.

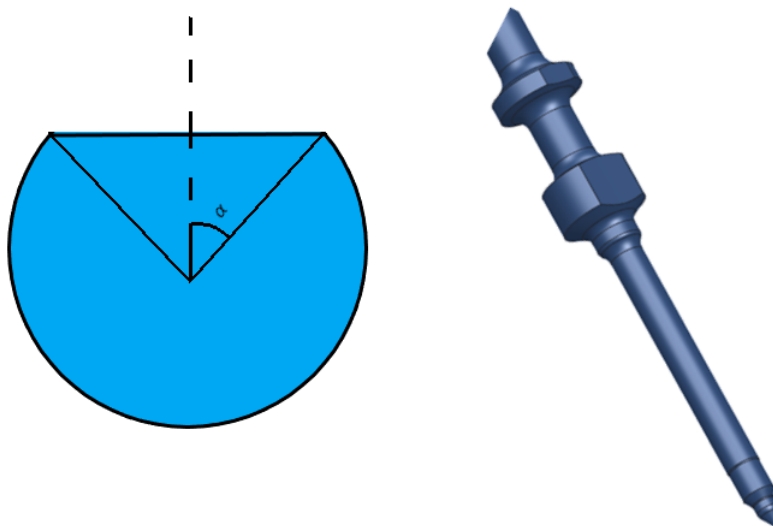


Figure 1.3: Flat gain orifice needle with the gain angle α . Courtesy of Cummins

1.4 Internal Diesel Injector Deposits

IDID's are usually a combination of two different deposits, one soap like deposit consisting of metal carboxylates and one polymeric amide forming a sticky plastic surface [4]. The formation of these deposits can result in higher fuel consumption or in worst case a ceased injector, both of which very undesirable.

The soap like metal carboxylates are believed to occur due to water and metal in the fuel, the water could come from sea transport or even from humid air while the metal could

come from transport, anti-corrosion inhibitors or from fatty bio-fuels. It is believed that the metal and water form reversed micelles [6][7] which can follow the fuel flow and when entering the injector the flow is so turbulent and the temperature is so high the micelle ruptures and the polar metal end can attach to the metal inside the injector and hence form a deposit.

To find and investigate IDID two different methods can be used, online testing and post test analysis.

1.5 Testing

When deposits form on the injector, its performance changes. Because of the low tolerances and high precision in the injector, even a small performance change can have large consequences. Engines with deposit issues have been found to have an increase in fuel consumption, a decrease in torque and in some cases even failed to start.

If the deposits can be produced in a controlled environment, at a much faster pace than in an engine a more detailed analysis of its mechanics can be studied. To do this a test rig is being built at Scania CV AB [8]. This rig uses a complete fuel system with a single injector which can be heated. The advantage of this is that tests can be done in a controlled environment with no regard for other engine components, with the goal of producing deposits and related injector problems for further analysis. To do this efficiently a well thought out test method must be used. To find a test method it is important to understand what changes can occur while the rig is running. This is referred to as online testing, whereas analysis after rig running is referred to as post test analysis. A fast and reliable production of IDID will mean a more comprehensive study of how deposits form and how to prevent their formation is possible.

1.5.1 Online testing

The first thing IDID change inside an injector is its geometry. Although not yet fully understood how these are formed the deposit will change the radius of both needle and sleeve. One other thing it could change is the surface roughness. Both of these phenomena can change the flow rate and the pressure drop when the needle opens. Measuring both of these can give a first indication of when IDID is starting to form. The small tolerances inside the injector means even a thin deposit will make a considerable change in the flow gap. With increased thickness the deposits in the sleeve and the needle can attach to each other increasing the friction of the needle, which will affect timing and needle stroke. It is when IDID stick together the engine can fail since the friction to lift the needle becomes larger than the lift force, hence ceasing the needle.

1.5.2 Post test analysis

A common approach to investigate IDID is to run an experiment until the injector has ceased and then brake it to analyse what has formed. Braking the injector is necessary since the inside of the sleeve needs to be analysed for deposits and is made of one cast piece. The tools used for analysis are for instance Fourier-Transform Infrared Spectroscopy (FTIR), Gas Chromatography-Mass Spectrometry (GCMS), Scanning Electron Microscopy (SEM) etc. In this way it is possible to find the composition of the material, thickness of deposits and other properties. The material composition is important to know because it gives a clue of where these deposits originate. Different methods are used in different experiments to find out more and more of what this is and where it is from.

2 Literature Review

What IDID do is building a layer in parts of the injector where it is hot. This is mainly in two places, the poppet where there are large pressure differences and fluctuations in gas content and flow and in the lower needle and sleeve where heat is transferred from the cylinder, where the needle is seen in fig 1.2. This project focuses on the needle, since most deposits have been found there. By looking at the fuel injection cycle as a closed system from the gain orifice and downwards the flow characteristics can be analysed from its geometry. Since the flow through this area is not fully understood two different approximations are used. One for laminar flow by using the Hagen-Poiseuille flow equation, and one where the flow is thought to be turbulent. By thinking of the system where a pressure pushes fuel out of the injector it is in this case interesting to look at the mass flow and how that changes with IDID and therefore no attempts of describing the turbulent fuel flow in detail is attempted.

2.1 Pressure drop

The outlet orifice in a fuel injector is designed to have a choking effect. This means that when the injector is fully open the pressure drop is only dependent on the total outlet area. This gives that early pressure changes is a sign of the nozzle holes decreasing in size. However if there are other signs that deposits are formed, such as timings, this could mean that the needle no longer can fully open and itself become the limiting factor in how much the pressure drops. In a testing rig, as well as field tests, it is hard to measure the pressure drop inside the injector. What can be done instead is to switch the high pressure pump off for a cycle and look at the pressure drop occurring in the common rail.

2.2 Temperature

In an engine the fuel is heated to a stable temperature from travelling through, for example, fuel pumps and cooling system before going in to the injector. Fuel exiting the injector has been heated by the cylinder while fuel entering the injector has not. This creates a temperature gradient inside the injector where the inlet fuel is about 80 °C and the fuel about to be injected can have a temperature of about 200 °C.

Studies have shown that IDID are formed at temperatures above 150 °C [9] which gives that areas close to the inlet in the injector should not be contaminated with IDID since that area is kept at about inlet temperature. The engine temperature can fluctuate due to different loads, engine breaking and fuel flows. This gives that the temperature gradient inside the injector can vary. This in combination with the fuel dynamics in the injector means the deposits do not distribute according to the temperature at the surface.

From Lacey et al. [6] it can be seen that if the flow is steady and there are no temperature or pressure fluctuations, deposits would be concentrated to temperatures above about 150 °C. A testing rig which is in between a steady flow test and an engine will behave more like an engine because when the injector is opening and closing pressure fluctuations occur moving fuel and deposits in the injector.

This means that deposits will probably form layers of representative thickness inside the injector since the soft particles that causes the deposits have a more Brownian motion than in the steady state test.

2.3 Formation of IDID

With bio-diesel mixed into diesel fuel new challenges occur, since bio-diesel consists of blends of Fatty Acids Methyl Esters (FAME) or Hydrotreated Vegetable Oil (HVO), both of which destabilize the fuel [5]. To keep diesel fuel usable for a long time additives are introduced, as well as both voluntary and involuntary particles in the form of, for example, salt, introduced from sea-water ballast during shipping or from salt dryers in refineries, sodium with alkenyl succinic acids, used as pipeline corrosion inhibitors, and lubrication additives [2] [10]. The different molecules form different kinds of particles where more common ones are metal soaps, polymeric acids, inorganic salts, aged fuel deposits, lacquers and carbonaceous [4] [11] [12]. The more common particles are the metal soaps which build up and cause changes in injector performance, as well as injector failures.

Although not fully understood how IDID are formed there are many hypotheses about it. Where most agree that IDID are sticky there are a few disagreements on the shape of its formation.

One hypothesis is that the deposit molecule sticks to the surface in the injector, collecting more and more molecules forming small grains that makes the surface rougher. After this the grains can connect and form an almost smooth layer. The "almost" part is important here because the layer can form small cracks, almost like peeled paint, which the fuel flow can grip and remove. If this is true a fuel flow difference should be seen

early from a changed relative roughness, however it might be very small.

Another hypothesis is that it simply forms a plastic film which is smooth and just increases in thickness. If that is the case there should be no variation other than a slow decrease in fuel flow as the deposit attaches [7].

Others have found that the deposits are often built up by particles smaller than the filter tolerances, meaning soft particles are probably produced in the fuel tank rather than in the injector [13].

Rounthwaite et al. [14] argues deposits form a smooth film while Bernemyr et al. [15] propose a mechanism to how the layers form inside an injector nozzle. This mechanism is based on the idea that small granules of metal carboxylates (metal soaps) are transported with the fuel where, in the heat and flow in the injector, they can attach to the surface. As more and more granules attach, a film is built up forming a layer, since these layers are not uniform, cracks can develop and parts of the deposits can detach from the surface. This can be thought of as similar to how icebergs break from an ice shelf, coasting away with the flow of the ocean. This mechanism is proposed for injector nozzles which environment is not dissimilar to the environment in the injector and will therefore be considered in this project.

2.4 Test fuel

To get a viable test fuel for experimenting, a method of creating soft particles is developed by Scania where a detailed description can be found in [16]. A summary of the method is that 10% bio-diesel, which is a diesel mix containing 10% bio-fuel and 90% diesel, is heated to 110 °C and stirred together with Calcium oxide for 72 hours. This ages the fuel mixture creating soft particle deposits in the bottom of the container which is separated and can be stored. The test fuel is made by mixing 0.5 g of these soft particles with 100 ml of 10% bio-diesel. When the liquid looks cloudy and the deposit drops are dissolved the mixture is determined finished and this fuel mix is added to 200 ml of 10% bio-diesel stirred and the test fuel is done.

3 Theory

A better understanding of how IDID affect injectors can lead to finding online test results in an experimental environment as well as finding clues of when deposits are formed. Comparing theory with field tests can be a mine field since theory usually isolates variables and assumes perfect conditions, whereas field test consist of vast amounts of variables such as an Electronic Control Unit (ECU) and driver which constantly regulates for example injector timings. Having a fully independent injector rig where all variables can be set is not very common and can be one of the reasons a theoretical background of how IDID affect performance has not been found in literature for this project.

3.1 Diesel properties

Flow, force balance and injector performance are heavily influenced by the properties of the liquid flowing through it. In this project the properties Swedish diesel [17] will be used for approximating the fuel in the injector. Due to the environment inside an injector of high pressures and high temperatures data is extrapolated with tools from Scania to give property values at 200 MPa and 200 °C. The properties of Swedish diesel at 200 MPa and 200 °C can be seen in table 3.1.

Table 3.1: Swedish diesel properties at 200 MPa and 200 °C.

Swedish diesel properties		
Property	Symbol	Value
Density	ρ	791.1 kg/m ³
Speed of sound	a	1607 m/s
Bulk modulus	B	2042 N/mm ²
Dynamic viscosity	η	6.175E-04 Ns/m ²

Since Swedish diesel contains 10% bio-diesel and this is the same fraction of bio-diesel in what has been seen causing IDID these are the properties used in this project. Cummins/Scania XPI injectors have an inbuilt characterisation system called Adaptive Injector Characterization (AIC) which drops the common-rail pressure to 50 MPa when testing. In a lab environment this can be used to look at injector performance and in those cases it makes more sense to analyse the results with diesel properties at 50 MPa and 200 °C which is shown in 3.2, however for the theory presented values at 200 MPa are used.

Table 3.2: Swedish diesel properties at 50 MPa and 200 °C.

Swedish diesel properties		
Property	Symbol	Value
Density	ρ	729,8 kg/m ³
Speed of sound	a	985 m/s
Bulk modulus	B	708 N/mm ²
Dynamic viscosity	η	5,387E-04 Ns/m ²

3.2 Fuel flow

When the injector needle opens fuel can start to flow into the cylinder. As long as the fuel is in-compressible the injection rate is a function of the injector's geometry and pressure difference between fuel pressure and cylinder pressure. From previous studies [18]

it can be seen that when the injector is opened it reaches its top position very quickly and stays there for the majority of time, until it closes where it, again, reaches its closed position very quickly. According to internal documents on fuel flow it can be seen that the acceleration phase of fuel is very short and for long injection periods this phase is negligible. Hence for long injection periods the fuel flow can be approximated as a steady state flow. With a steady-state flow the injection rate is dependent on the geometry inside the injector, where some have found it to be laminar and others found it to be turbulent, both of which are dependent on geometry and therefore deposit thickness but with variations in how much it affects the injection rate.

3.2.1 Laminar flow

From fluid mechanics [19] a general expression for an in-compressible fluid can be written by the Navier-Stokes equation as

$$\rho \frac{d\bar{u}}{dt} \equiv \rho \left[\frac{\partial \bar{u}}{\partial t} + (\bar{u} \cdot \nabla) \bar{u} \right] = -\nabla p + a \nabla^2 \bar{u}, \quad (3.1)$$

where ρ is the density, \bar{u} is the velocity vector, p is the pressure and a is a constant independent of pressure and velocity. From a steady state flow it is seen that all time-dependence is zero. Furthermore if the flow is laminar which means there is no turbulence of the flow which gives $(\bar{u} \cdot \nabla) \bar{u}$ is zero. The constant a is a property of the fluid and is found to be its viscosity η , which gives the following equation:

$$-\nabla p + \eta \nabla^2 \bar{u} = 0. \quad (3.2)$$

The flow velocity is now a function of the geometry, viscosity and the pressure gradient ∇p . With a no slip boundary condition in a circular cross-section the Navier-Stokes equation can be written as

$$\frac{1}{r} \frac{\partial}{\partial r} \left(r \frac{\partial u}{\partial r} \right) = \frac{1}{\eta} \frac{dp}{dz} \quad (3.3)$$

where z is in the axial direction and r is in the radial direction, η is the dynamic viscosity of the fuel. The pressure gradient, $\frac{dp}{dz}$, can be rewritten as $\frac{\Delta p}{L}$ where Δp is the pressure difference between the inlet and the outlet and L is the length of the geometry. By approximating the injector as an annular cylinder with boundaries R_1 and R_2 the Hagen-Poiseuille equation gives

$$u(r) = \frac{\Delta p}{4L\eta} \left((r^2 - R_1^2) - (R_2^2 - R_1^2) \frac{\ln(r) - \ln(R_1)}{\ln(R_2) - \ln(R_1)} \right). \quad (3.4)$$

This equation gives the flow velocity at different radii and Δp is the pressure drop over the length L . To be able to compare theory with experiments the volumetric flow rate is considered. By looking at the average fuel flow through a cross section of the cylinder the volumetric fuel flow becomes

$$Q = \frac{\Delta p \pi}{8L\eta} \left[R_2^4 - R_1^4 - \frac{(R_2^2 - R_1^2)^2}{\ln(R_2) - \ln(R_1)} \right]. \quad (3.5)$$

The volumetric Hagen-Poiseuille flow is a steady state flow for a laminar case. If the flow inside an injector is laminar this could approximate an injection cycle for long injection times since acceleration rates can be neglected and the fuel flow can be seen as steady state. When deposits are formed the radii R_2 and R_1 will decrease and increase respectively forming a smaller and smaller channel for fuel to pass.

3.2.2 Turbulent flow

With turbulent flow a different approach for the fuel flow is needed. From the Darcy-Weisbach equation [20] the pressure-loss form is

$$\Delta p = f_d \frac{L}{D_h} \frac{\rho \langle v \rangle^2}{2}. \quad (3.6)$$

This form is for an annulus with hydraulic diameter D_h and length L , with the the Darcy friction factor f_d and mean velocity $\langle v \rangle$. The hydraulic diameter for an annulus is found by

$$D_h = \frac{4A}{P} = D_2 - D_1 \quad (3.7)$$

where A is the cross-sectional area, P is the wetted perimeter given by $\pi(D_2 + D_1)$ and D are the different diameters. Rearranging (3.6) for velocity it becomes

$$\langle v \rangle = \left(\frac{2\Delta p D_h}{\rho L f_d} \right)^{1/2} \quad (3.8)$$

which gives the mean velocity in the geometry. The volumetric flow is found by multiplying the former equation with the cross-section area. This means

$$Q = A \langle v \rangle. \quad (3.9)$$

The only unknown factor is now f_d . This factor is found with the Colebrook-White equation

$$\frac{1}{\sqrt{f_d}} = -2 \log \left(\frac{\epsilon}{3.7 D_h} + \frac{2.51}{Re \sqrt{f_d}} \right) \quad (3.10)$$

which is an implicit equation. The numbers are found from empirical testing, ϵ is the roughness of the material and Re is the Reynolds number defined by

$$Re = \frac{Q \rho D_h}{\eta A} \quad (3.11)$$

where η is the dynamic viscosity. This gives the following system of equations

$$\begin{cases} Q = A \left(\frac{2 \Delta p D_h}{\rho L f_d} \right)^{1/2} \\ \frac{1}{\sqrt{f_d}} = -2 \log \left(\frac{\epsilon}{3.7 D_h} + \frac{2.51}{Re \sqrt{f_d}} \right) \\ Re = \frac{Q \rho D_h}{\eta A} \end{cases} \quad (3.12)$$

where it is seen that volumetric fuel flow and Reynolds number are dependent on each other and the friction factor is implicit. By using a Moody diagram and looking at the Reynolds number in the base case, it can be seen that the flow is in the turbulent zone. In this zone the friction factor can be approximated as a constant which eliminates the need for an implicit solver to find the friction factor. However the fuel flow inside of the injector is, due to the high pressures, compressed and therefore not determined by the Darcy-Weisbach equation. Even with severe deposits in the injector the orifice area in the gain orifice is larger than the nozzle orifice area, which is the limiting flow factor. However if needle movement is limited, this could end up limiting the fuel flow to the cylinder.

3.2.3 Compressible flow

Even if liquids are normally considered to be in-compressible the properties of a liquid changes when the pressure differences are high enough. Under high pressures a liquid is better described as compressible and the flow characteristic changes. Neither laminar nor turbulent flow equations can fully describe the flow. In hydraulics, such as fuel in an injector, a choking effect can occur, either by design or by accident. The choking effect occurs when a pressure drop is so high that the fluid is accelerated to its sonic speed. When this happens the flow velocity is no longer dependent on increased pressure differences or geometry [20]. A choking effect is designed to occur from the nozzle holes in the injector and changes in mass flow is only from density differences. With density being dependent on pressure and temperature, and those two characteristics being independent on IDID, finding injector performance changes from IDID build-up must be considered improbable.

A change in pressure drop, from deposits, at the common rail as the needle opens is minuscule. This means finding injector performance changes from IDID build-up is almost impossible.

3.3 Shear force

The shear force is the shear stress from the flow integrated over the area on the side of the needle surface. Due to the special geometry of the flat gain orifice it is hard to know what kind of flow is flowing past it which is where the problems with deposits are suspected to form. By testing with solving Poiseuille flow and drawing some characteristics from that, together with literature, some qualified guesses of the deposits impact can at least be made. The Poiseuille flow through the bearing is found from

$$\frac{\partial^2 u}{\partial r^2} + \frac{1}{r} \frac{\partial u}{\partial r} + \frac{1}{r^2} \frac{\partial^2 u}{\partial \phi^2} = \frac{1}{\mu} \frac{\partial p}{\partial z} \quad (3.13)$$

where $u = u(r, \phi)$ is the velocity vector, r is in the radial direction, ϕ is in the angular direction. By following the method presented by Alassar [21], approximating $\frac{\partial p}{\partial z}$ as the pressure drop in the injector Δp and introducing a dimensionless velocity $\omega(R, \Theta) = u / (\frac{R_1^2 \Delta p}{\mu})$, the problem can be written as

$$\frac{\partial^2 \omega}{\partial R^2} + \frac{1}{R} \frac{\partial \omega}{\partial R} + \frac{1}{R^2} \frac{\partial^2 \omega}{\partial \Theta^2} = -1 \quad (3.14)$$

with a particular solution as

$$\omega_{\text{particular}} = -\frac{R^2}{2} \sin^2 \Theta. \quad (3.15)$$

The homogeneous equation left is

$$\nabla^2 \omega_{\text{homogeneous}} = 0 \quad (3.16)$$

which is the Laplace equation solved by

$$\omega_{\text{homogeneous}}(R, \Theta) = A + B \ln(R) + \sum_{n=1}^{\infty} \left(A_n R^n + \frac{B_n}{R^n} \right) [C_n \cos(n\Theta) + D_n \sin(n\Theta)] \quad (3.17)$$

with the complete solution $\omega(R, \Theta)$ being the sum of the particular and homogeneous function. The no slip boundary conditions are as follows:

$$\begin{cases} \omega(R = R_2, \Theta) = 0 \\ \omega(R = R_1, \alpha < \Theta < 2\pi - \alpha) = 0 \\ \omega(R = R_1 \cos \alpha, -\alpha < \Theta < \alpha) = 0 \end{cases} \quad (3.18)$$

where α is the angle from the center line through the origin and center of the flat surface and the edge of the flat surface, seen in fig 1.3. The shear stress from the fluid flow is a function of the viscosity and velocity gradient and is defined as

$$\tau(y) = \mu \frac{\partial u}{\partial y} \Big|_{y=0} \quad (3.19)$$

where y is represent the distance to the surface and $y = 0$ therefore is the surface. As shear stress is dependent on the velocity gradient and for smaller gaps the flow velocity must be higher to reach the same volumetric flow, it can be concluded that the shear stress is larger for smaller gaps. This gives that in an injector the shear stress is highest where the gaps are smallest which is the flat gain orifice 1.3. Since deposit build-up decreases the gap, shear stress increase as IDID attach to the surface of the injector. For turbulent flow the friction factor can be used and the shear stress is written as

$$\tau = f_d \frac{8Q^2}{\rho A^2}. \quad (3.20)$$

Here A is the area where the flow occurs and as this decreases because of deposits it is seen that the stress increases, which is expected. The friction factor is dependent on surface roughness and it is therefore important to be careful when considering its value, the roughness increases with deposits. However the significance this has on the shear stress is small and can be considered as a carefully chosen constant[20]. The total shear force is the shear stress integrated over the surface area, S , on which the stress acts, which gives

$$F_{shear} = \oint_S \tau dS. \quad (3.21)$$

The surface area is the area of interest to find the total force, in this case it is that of the needle since it has to move in an injection. For a large part of the injector the area between the needle and sleeve is an annulus. The flat gain orifice the surface is a bit more complicated and gives flow area as

$$A = \pi R_2^2 - \alpha R_1^2 - \frac{R_1^2}{2} \sin(2\alpha) \quad (3.22)$$

where α is the angle to the from the center of the needle to the edge of the flat plane, which can be seen in fig 1.3. The surface area, S , where the shear force is acting is described by

$$S = 2LR_1(\alpha + \sin(\alpha)) \quad (3.23)$$

where L is the length of the flat gain orifice. Now the fuel flow Q is set to be constant, which in real cases it is not when deposits occur. However with the different geometry the Reynolds number and Darcy friction-factor changes in that the hydraulic diameter D_h changes with

$$D_h = \frac{\pi R_2^2 - \alpha R_1^2 - R_1^2 \sin(2\alpha)}{\pi R_2 + \alpha R_1 + R_1 \sin(\alpha)}. \quad (3.24)$$

The shear force also affects the lower part of the needle where the flow area is approximated as an annulus, $A_{annulus}$, which gives the the surface area, $S_{annulus}$, of the lower part of the needle and the hydraulic diameter $D_{h,annulus}$ as

$$\begin{aligned} A_{annulus} &= \pi(R_4^2 - R_3^2) \\ S_{annulus} &= 2L_{annulus}\pi R_3 \\ D_{h,annulus} &= 2(R_4 - R_3) \end{aligned} \quad (3.25)$$

where R_4 , R_3 and $L_{annulus}$ are the outer radius, inner radius and length of the lower part of the needle. The total shear force at the needle can then be written as

$$F_{shear} = f_d \frac{8Q^2}{\rho} \frac{S}{A^2} + f_{d,annulus} \frac{8Q^2}{\rho} \frac{S_{annulus}}{A_{annulus}^2} \quad (3.26)$$

which with dimensions becomes

$$F_{shear} = \frac{8Q^2}{\rho} \left(f_d \frac{2LR_1(\alpha + \sin(\alpha))}{\left(\pi R_2^2 - \alpha R_1^2 - \frac{R_1^2}{2} \sin(2\alpha)\right)^2} + f_{D,annulus} \frac{2L_{annulus}\pi R_3}{(\pi(R_4^2 - R_3^2))^2} \right) \quad (3.27)$$

where f_d is a function of the hydraulic diameter D_h . By testing setting an initial gap of 0.5mm at the flat gain orifice (which is larger than the real injector) and plotting the shear force as a function of the remaining flow gap in percentage of the original the result can be seen in figure 3.1. What is not seen is that this graph shows results of different angles of cut-out, α , which means that as soon as there is a considerable gap where fuel can flow almost all mass pass there and not in the thin gaps. This gives that changes in shear force due to different angles are very small and not considered. What also can be seen is that the forces are in tens to hundreds of micro Newtons, which are about a hundred thousand times less than the lifting force. Therefore it is concluded that injector performance changes will only be detectable when the deposits either are sticking together, introducing friction, or if IDID create an increase in viscosity.

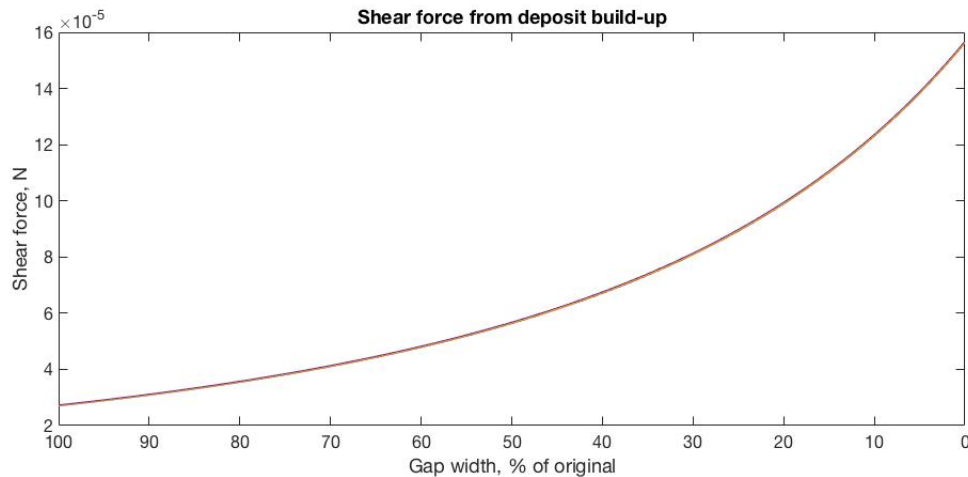


Figure 3.1: Shear force from fluid on needle with decreasing gap between needle and sleeve.

Since IDID is almost toffee like in its texture it can be seen as a highly viscous fluid. As IDID starts to stick together a simple approximation would be that the viscosity changes since deposits have a much higher viscosity than diesel. If there is a change in viscosity the variable in (3.20) is the Darcy friction-factor f_d . As seen in (3.12) the factor is dependent on the Reynolds number which is inversely proportional to the viscosity η . By plotting an increasing viscosity to shear force it can be seen that this is much more likely to affect injector performance, however the viscosity of IDID is unknown and viscosity build-up is also an unknown factor. It is important to note that shear force from viscosity is not to be confused with friction since the shear force will resist upward movement, against the fuel flow, but help downward movement, with the fuel flow, which can show itself in an increased opening time but decreased closing time for a needle. Whereas friction will resist any movement.

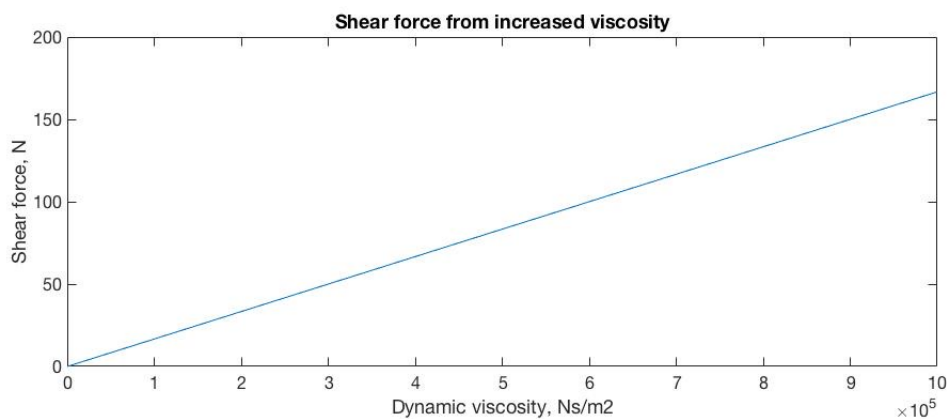


Figure 3.2: Shear force from fluid on needle with an increase in viscosity.

3.4 Friction

Tanaka et al. [22] found that injection rate changes as deposits affect the injector. What they found was that the beginning of injection is slower whereas the End Of Injection (EOI) is delayed. From an approximation of friction where

$$F_{fric} = -\mu N \quad (3.28)$$

it is seen that this force is only dependent on the normal force, N , and a friction factor μ . Because of rotations, flow and needle bending in its motion it is very difficult to find an accurate model for the normal forces. An alternative way to look at the friction forces is to look at the dynamics of the needle, to look at the needle's position as a function of time. With deposits the main change in friction will come from the friction factor which increases, a property of a material being sticky, the friction force is therefore approximated as a linear function of the friction factor μ . One way to find the effect of friction is to treat N constant force on the needle, since, in general, deposits should not affect the normal force inside the injector.

3.5 Drag force

With fuel flow having a velocity a drag force is present. This force can be seen as the flow hitting an object which is perpendicular to the flow, which is why a frontal area is often used as a reference to find the total drag. In this case bio-diesel will hit the flat gain orifice where the fuels kinetic energy is the mass of the fuel hitting multiplied by the velocity of the fuel squared. The force this energy then affects the orifice with is dependant on the frontal area and a drag coefficient dependent on the geometry of the orifice and Reynolds number. In this case the Reynolds number is high enough for the drag coefficient to be constant. This drag force can be seen as

$$F_{drag} = \frac{1}{2} \rho u^2 C_d A' \quad (3.29)$$

where C_d is a constant dependent on geometry, that after discussion is set to 0.82 and A' here being the frontal area of the needle. This frontal area is approximated as the cross-sectional area of the flat gain orifice, which is the blue area in fig 1.3. With deposit build-up the frontal area increases slightly together with the decrease in gap between needle and sleeve. The changes from deposits are mainly from density and flow area differences, where the decrease in tolerances from deposit build-up decreases the flow area, resulting in a higher velocity. Rewriting the drag equation with volumetric flow the equation becomes

$$F_{drag} = \frac{1}{2} \rho \frac{Q^2}{A^2} C_d A'. \quad (3.30)$$

From 3.22 the flow area is known, the frontal area becomes the part of the equation dependent on R_1 which means with changes in build up the drag force is

$$F_{drag} = \frac{1}{2} \rho C_d Q^2 \frac{\alpha R_1^2 + \frac{R_1^2}{2} \sin(2\alpha)}{(\pi R_2^2 - \alpha R_1^2 - \frac{R_1^2}{2} \sin(2\alpha))^2}. \quad (3.31)$$

From plotting the drag force as a function of deposit build up the force can be seen in figure 3.3.

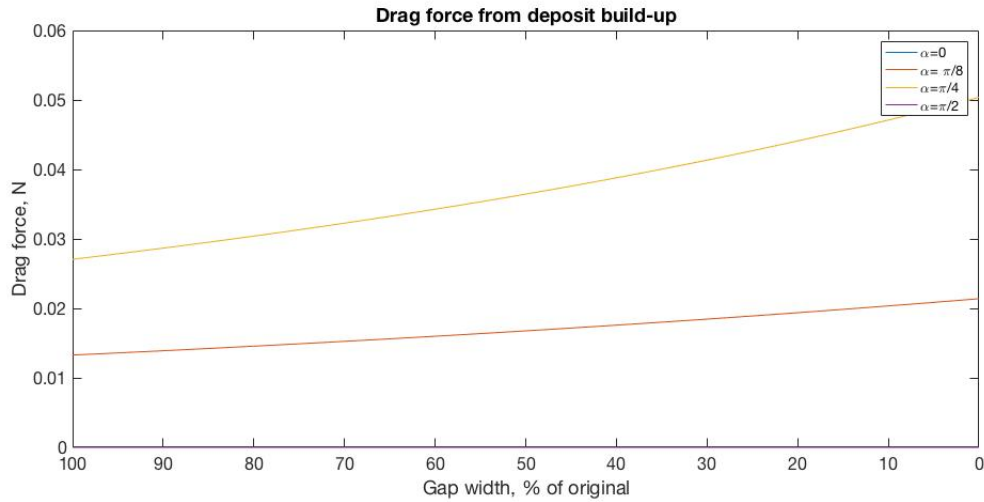


Figure 3.3: Drag force as function of deposit build up for a flat gain orifice.

The different forces seen in fig 3.3 is due to different angles of the flat gain orifice which means the frontal area varies. For a reasonable injector the upper graph, in yellow, can be used.

3.6 Joukowsky pressure

A risk of all hydraulic systems is the build up of pressure due to fast closing of a valve. When a valve is closed rapidly the moving fluid hits a wall and is stopped instantaneous. This causes a back pressure traveling upstream which can cause disruptions and even failure of the system [23]. The pressure difference for an ideal case is described by

$$\Delta P = \rho a \Delta v \quad (3.32)$$

where ΔP is the pressure difference caused by instant closing of the valve, ρ is the density of the fluid, a is the speed of sound in the fluid and lastly Δv is the velocity change of the fluid, in this case the volumetric velocity divided by the flow area, since the fluid stops. Putting this in numbers where data is found in table 3.1 and $\Delta v = Q/A = 8.31$ m/s gives that the maximum Joukowsky pressure for a normal injector would be 11.3 MPa, which is about 5.7% of the common rail pressure. A risk with fast closing of the needle

is that the Joukowsky pressure travels to the back wall, in this case the flat gain orifice, is reflected and travels back to the needle closure where a new pressure is produced creating a resonance shock wave which adds the Joukowsky pressure in altitude for each cycle. For this to happen the time between closing the needle must be the same time it takes for the shock wave to travel from the needle closure, to the flat gain orifice and back again. The shock wave travels at the speed of sound in the diesel and the time T it takes for it to travel is

$$T = 2\frac{L}{a} \quad (3.33)$$

where L is the length of the needle closure to the flat gain orifice. Putting numbers in this for a healthy injector yields the time needed for the pressure to get back to the needle closure is $25.5 \mu\text{s}$. The injector is normally open for about 1ms and closed for about 20 ms which gives that even in unrealistic scenarios where one cycle is open for 1 ms and closed for 1 ms , the shock wave has still been able to travel back and forth almost 40 times while the needle is closed. At that point the shock wave has been dampened enough to become negligible and the risk of failure because of Joukowsky pressure is also negligible.

3.7 Needle dynamics

In fig 3.4 the different areas responsible for the needles dynamics can be seen. When the injector is activated a small poppet, yellow in figure 3.4, is lifted creating a low pressure area in the control chamber, P_{CC} . The pressure difference $P_s - P_2$ is designed with the flat gain orifice and is there to slow down opening and helping closing the needle. When the needle closes the poppet drops to its seat increasing P_{CC} to the common rail pressure P_s removing the low pressure area and lets the spring and flat gain orifice close the needle. When the needle is in its bottom position the spring pushes the needle down which is counteracted by the normal force from the sleeve. However for the needle dynamics this normal force is zero as soon as the needle starts to lift and therefore the force balance in the injector can be written as

$$P_{sac}A_4 - (P_s - P_2)A_3 - P_2A_4 + P_sA_2 - P_{CC}A_2 - F_{spring} = ma \quad (3.34)$$

where P_{sac} is the pressure in the nozzle and $A_1 - A_4$ are the different areas in the injector. This is all with the positive direction as up in fig 3.4. The result ma is the mass of the needle times the needle acceleration from Newtons laws. As the needle opens the spring force increases and when the sum of the net force pulling the needle up, the flow forces and the spring force, is zero the needle enters a hovering state which is its uppermost position. In a healthy injector this is seen as its fully open position.

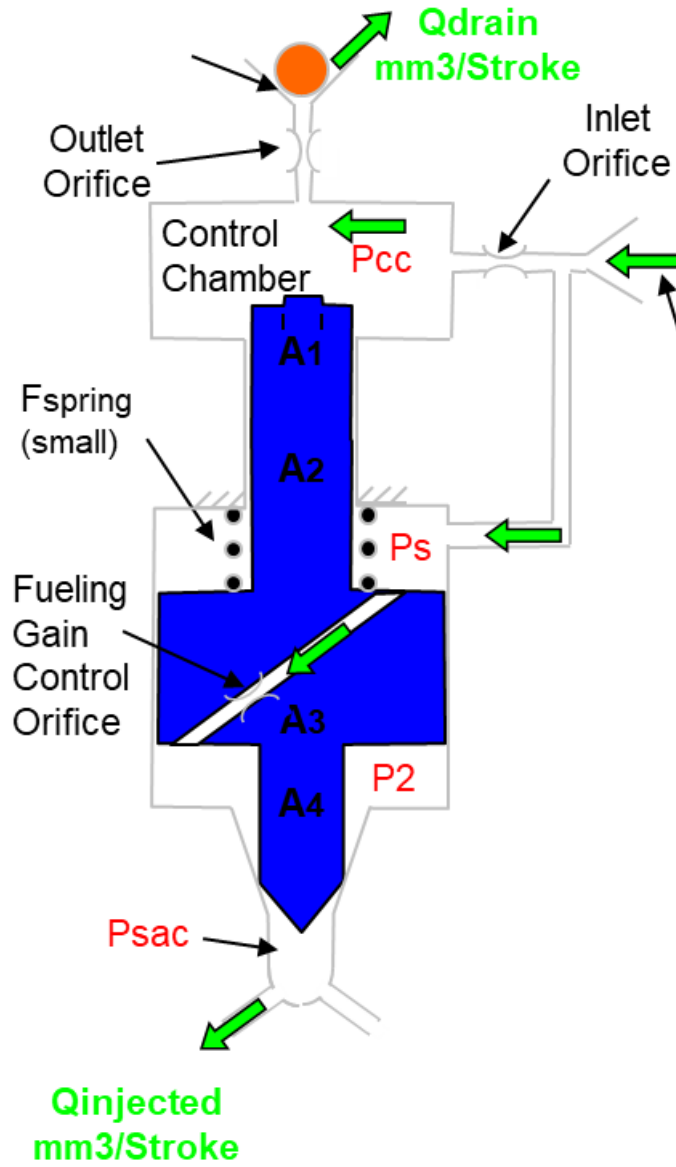


Figure 3.4: Force schematic over an injector. Courtesy of Cummins.

When deposit builds up in the injector the force balance is changed and drag, shear and friction forces are introduced. The total shear force for the moving needle is

$$F_{shear,needle} = f_d \frac{8}{\rho} \left(v_{needle} + \frac{Q}{A} \right) \left| v_{needle} + \frac{Q}{A} \right| 2LR_1(\alpha + \sin(\alpha)) \quad (3.35)$$

where A is the flow area described from (3.22) and v_{needle} is the velocity of the needle. The same thing can be seen for drag force where

$$F_{drag,needle} = \frac{1}{2} \rho C_d \left(v_{needle} + \frac{Q}{A} \right) \left| v_{needle} + \frac{Q}{A} \right| \left(\alpha R_1^2 + \frac{R_1^2}{2} \sin(2\alpha) \right) \quad (3.36)$$

which gives that the drag force is dependent on both the needle velocity as well as the flow velocity. In both cases the volumetric fuel flow is downwards in the injector

which means when the needle is opening the forces increase and as it closes the forces first decrease until the needle velocity passes the flow velocity, when the force again increases. When deposits between needle and sleeve starts to stick together a friction is introduced, from (3.28) this force is seen as a constant normal force with a friction factor. By introducing a new friction factor μ' , which is a variable dependent on the amount of deposits, the friction can be written as

$$F_{friction} = -\mu' N. \quad (3.37)$$

The new dynamic for the injector with deposits is therefore

$$P_{sac}A_4 - (P_s - P_2)A_3 - P_2A_4 + P_sA_2 - P_{CC}A_2 - F_{spring} - F_{shear,needle} - F_{drag,needle} + F_{friction} = ma. \quad (3.38)$$

4 Methodology

A lot is unknown about how deposits are formed, the properties and dynamics of IDID formation and no standard testing procedure is available. In field testing as well as some laboratory rig testing the test period is usually in the range of several weeks. Even if this can be an acceptable amount of time an accelerated test is preferred since it can give more results in the same amount of time. To find a fast and reliable test-cycle there are some properties of IDID that need to be considered. To have enough IDID in the injector it is important to have a fuel flow that brings IDID particles with it. If only this was needed it would mean the fastest way to produce IDID are to open the injector and just let fuel flow through. Another aspect is that the deposits could need both time and heat to form and attach to the injector surface and if this is true the best way to do that is by closing the injector, contradicting the demand for a flow. As it is also unknown if the deposits are susceptible to tearing from the surface the ratio between time when open and time when closed could be of importance, a short time closed could not only cause that deposits will not form because of no time to attach but also high accelerations in the injector might just rip the deposits from the surface.

After discussions about limitations the consensus is that an injector in this regard is super robust to unrealistically high frequencies (which would simulate an engine running well above its maximum rotational speed), the risk of a water-hammering effect is negligible since those forces are much smaller than forces involved in opening and closing of the injector. The biggest risk would be to damage the electromagnet since it handles high amounts of current when switched on, however it is also continuously cooled which lowers the risk of this happening significantly. The limitations when testing in rig is therefore much more probable to come from other components in the fuel system.

4.1 Screen test

A screen test is a common method for testing fuel. It generally consists of letting fuel flow through a heated pipe in order to analyse what happens to the chemical composition of the fuel in the fueling system. To find a suitable fuel for the test rig a modified screen test is carried out. This test follows the theory from [6] but the method is simplified where instead of creating a temperature gradient, the fuel is instead tested for different temperatures. In the test an injector is put in two different containers with 10% Bio-Diesel (B10), a fuel mixture of 10% bio-diesel and 90% diesel, with added soft particles,

where one container is open to air and evaporation whereas the other container is recirculated so the diesel vapour is cooled and returns to the container. The first test is to heat these containers to 110 °C with a stirring of 550 RPM to keep the fuel uniform. After 24 hours the set up is turned off and the fuel is allowed to cool down before removing the injectors. A second test is done in mostly the same way where the temperature is changed to 150 °C before the fuel is left to cool for an extra 24 hours before examining the injectors. A third test is made in the same way as the second, but with a steady air flow to further oxidise the bio diesel as it is heated. After a visual inspection the deposits, if there are any, are measured in an FTIR to find the chemical composition.

4.2 Test rig

An injector test rig has been designed and will be set-up at Scania CV AB. This rig uses a pump system, common-rail and cylinder-head from a Scania truck. A detailed work of this can be found in a master thesis by Ashna [8]. From figure 4.1 the rig works as following:

1. B10 with added soft particles is stored in a fuel tank (1), where it is continuously circulated by the circulation pump (6). This is to keep the test fuel uniform.
2. A low pressure pump (2) feeds fuel from the fuel tank (1) through a flow meter (3) to the high pressure pump (4).
3. The high pressure pump (4) raises the pressure and feeds it to the common rail (7). Excess fuel is returned to the fuel tank (1) via a heat exchanger (5).
4. From the common rail (7) the fuel reaches the injector (8) where a heater (9) and a thermometer (10) are attached.
5. Fuel is injected from the injector (8) into a collection cup (11). The fuel then passes through a heat exchanger (12) before reaching the spill tank (13).

The advantage with a test rig is that experiments can be conducted in a controlled environment where fuel pressure and temperature can be regulated. Also there is no need to take other engine components into consideration, which means unrealistic scenarios can be tested which is vital for conducting accelerated tests. A more subtle advantage is that in running engines the fuel injector cycle is continuously modified by the ECU which reads data from different sensors to adjust engine performance. In a rig the ECU can be set to run with a test protocol with set variations to the injection cycle as well as continuously measure fuel flow and common-rail pressure.

The fuel flow in this rig is measured by a flow meter attached to the fuel tank which can give a quantitative result of fuel flow variation for longer time periods. Attached to the common rail is a pressure gauge which can monitor pressure variations over time. In

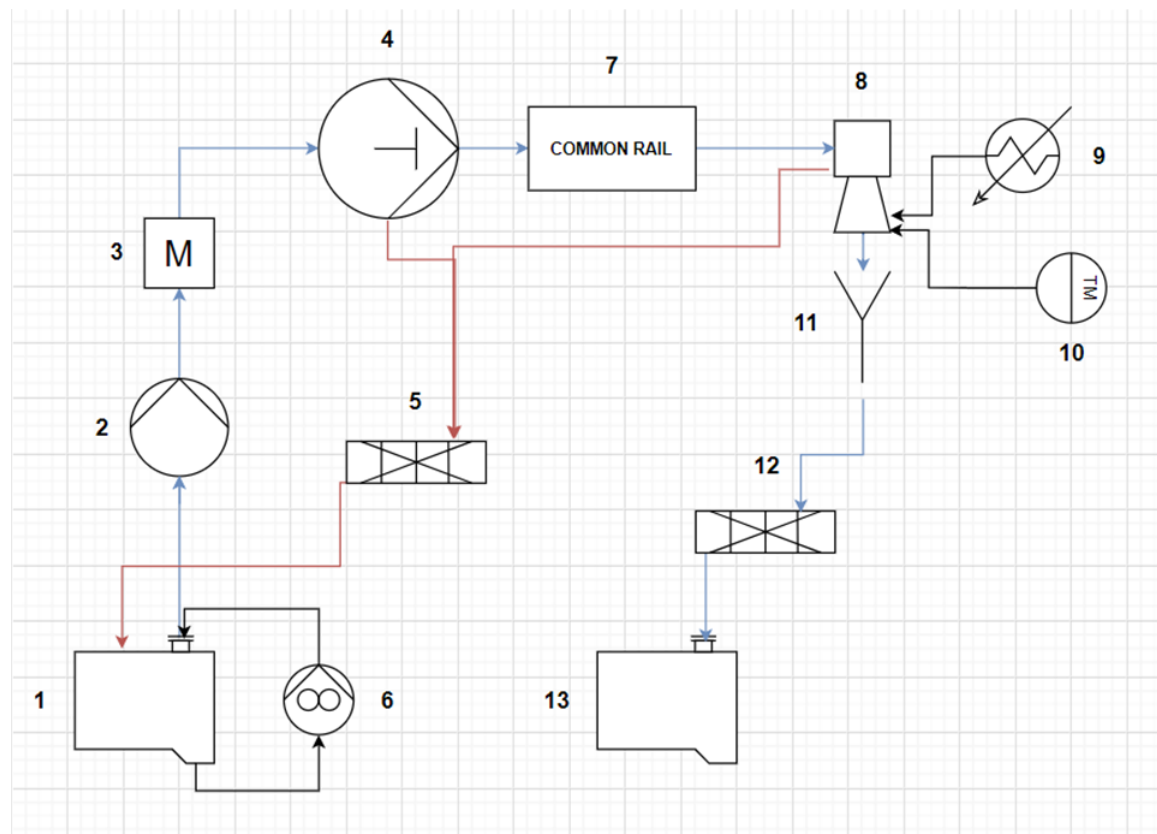


Figure 4.1: System overview over the test rig. 1) Fuel tank, 2) Low pressure pump, 3) Flow meter, 4) High pressure pump, 5) Heat exchanger, 6) Circulation pump, 7) Common rail, 8) Fuel injector, 9) Heater, 10) Thermometer, 11) Collection cup, 12) Heat exchanger, 13) Spill tank. Figure from Ashna [8].

engines this is one component that works together with the ECU to adjust the injectors. In a rig this can be used to not only look for pressure changes as IDID affect the injector, it can also be used to look for injector timings. This is done by the built-in AIC which lowers the high pressure pump's pressure for a few cycles and measures the pressure variation for when the injector opens respectively closes.

The heater in the rig is made from a ceramic material and has been fitted to the injector by modifying a cylinder head so that the heater is in close proximity to the lower part of the injector sleeve. The thermometer is attached to the heater which means that the temperature read-out is from there and not from the fuel temperature. To run experiments a modified injector, containing a thermometer, must first be used to see the temperature difference between the heater and the fuel.

By using B10 with a high concentration of soft particles in the rig and running it with a set test protocol a accelerated test can be conducted. Where fuel flow and needle dynamics can be continuously measured which can be used to find how and when IDID affect injector performance.

5 Results

5.1 Screen test

After a visual inspection of the injectors after the screen test at 110 °C no deposits were found and those needles were reused for the first test at 150 °C. The injector needle from testing in an open container at 150 °C can be seen in fig 5.1 where the slightly yellow colour is evidence of deposits.

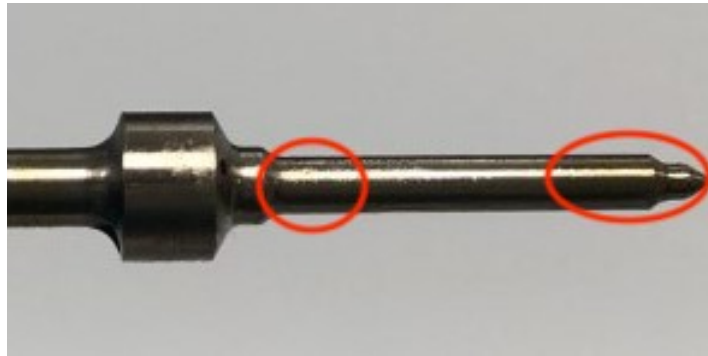


Figure 5.1: Visual inspection of needle from testing at 150 °C in an open container. IDID are circled in red.

The needle inside the closed container at 150 °C can be seen in fig 5.2 and it is seen that there are less deposits compared to the open container.



Figure 5.2: Visual inspection of needle from testing at 150 °C in a closed container. IDID are circled in red.

Lastly the needle inside a closed container with an airflow through the bio diesel is seen in fig 5.3 where a lot of deposits can be seen.



Figure 5.3: Visual inspection of needle from testing at 150 °C in a closed container with air flow. IDID are seen as a yellow like colouring on the needle.

From visual inspection some deposits were scraped off for analysing with FTIR. FTIR uses an infrared beam to find how much a test object absorbs for each wavelength. By using this method for hydrocarbons the wavelengths absorbed tells the length of the hydrocarbons, which can be used to find the chemical composition. In the case of the needle with a closed container the deposits were not enough to analyse. The results in figure 5.4 and figure 5.5 shows the percentage of light reflected by the test sample at each wavelength⁻¹. For the open container the FTIR analysis can be seen in fig 5.4, where the peak at 1605 cm⁻¹ is the peak of metallic soap particles. The closed container with air flow can be seen in fig 5.5, where again the peak at 1606 cm⁻¹ is from metallic soap particles.

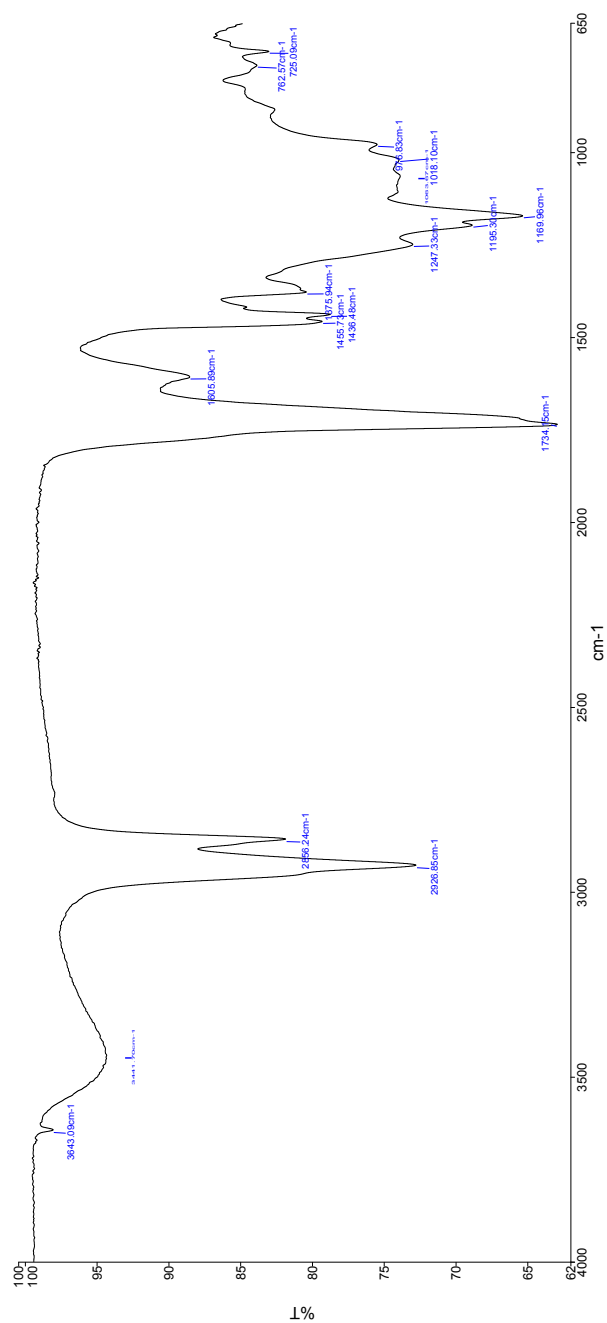


Figure 5.4: FTIR from open container at 150 °C. Shows percentage of infrared light reflected by test fuel for each wavelength⁻¹. Signs of IDID at 1605 cm^{-1} .

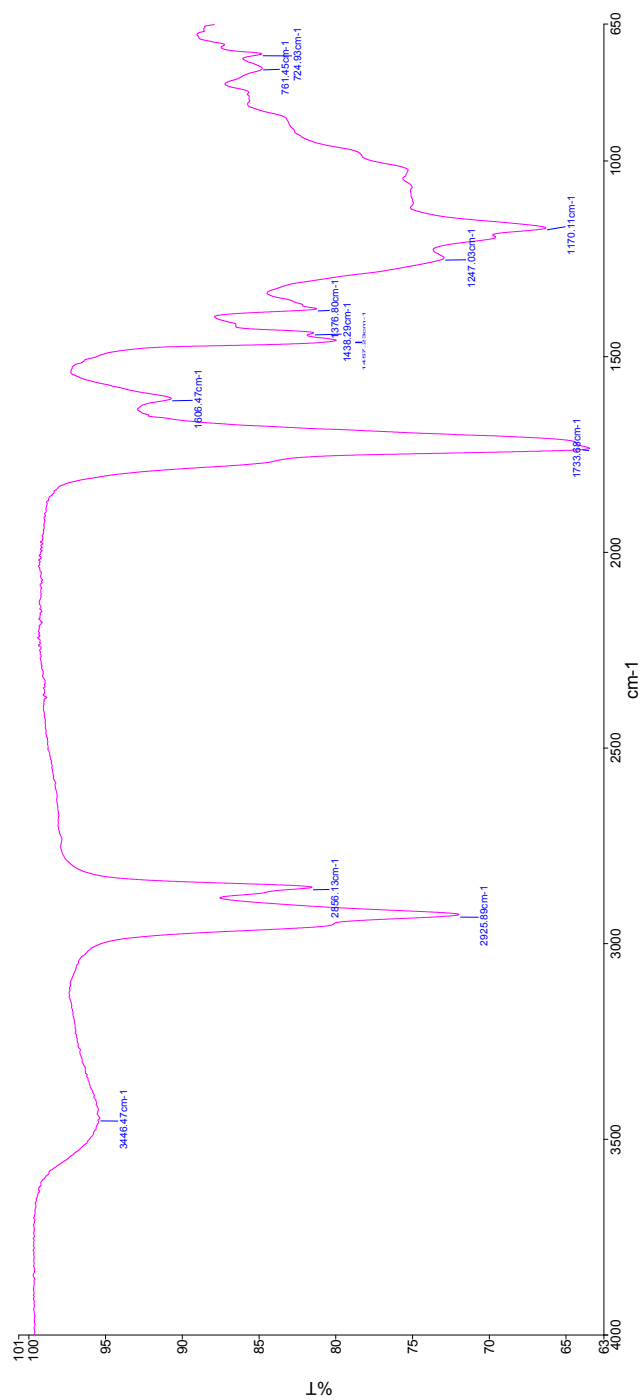


Figure 5.5: FTIR from closed container with air flow at $150\text{ }^{\circ}\text{C}$. Shows percentage of infrared light reflected by test fuel for each wavelength $^{-1}$. Signs of IDID at 1606cm^{-1} .

6 Discussion & Analysis

6.1 Screen test

The screen test of the fuel yielded the results predicted by [6] where no deposits were found at 100 °C while deposits were found at 150 °C. From FTIR it also showed that the deposits formed on the needles were the same metallic soaps that were added to the fuel to create a valid testing fuel, this shows that there is no chemical reaction at higher temperatures forming new particles that become the deposits, much like the authors of [15] discuss in their report.

6.2 Needle dynamics

Due to time constraints and software issues a result from needle dynamics because of deposit build-up and friction are not available. However there are a few conclusions that can be found from analysing the forces and how they change due to deposits.

As can be seen in (3.36) and (3.35) the drag and shear force are always acting in the same direction and can therefore be added together, from fig 3.3 and fig 3.1 it can be seen that the drag force in the static case is about ten times higher than the shear force, which means when deposits are building the main force affecting the needle is the drag force, although these forces are still very small compared to lifting forces from design of the injector. If the shear and drag force has a noticeable effect on the injector performance as deposits form this will be seen as a lower terminal speed for the needle when opening and a higher terminal speed when closing. This would mean a lower total fuel injection for each cycle and a total decrease in fuel flow, it would also mean that pressure drop in the common-rail would be more gradual when opening and have an earlier EOI.

The shear force presented in fig 3.2 shows much higher forces and if this is what happens in an injector it would show a large change in terminal velocities where opening would be extremely slow while closing would be almost instant, unless the needle velocity is higher than the flow velocity, in which case the shear force would slow down the closing. This is not what has been seen by Tanaka et al. [22] where they found EOI delays. Also considering how sticky the deposits are this approximation is not viable, because of its stickiness it would act to reduce movement in any direction. This gives the most

probable force to affect the injector dynamics is friction which comes from deposits.

In a healthy injector the small tolerances in the flat gain orifice helps create an almost friction-less environment, when the deposit layer is thick enough for needle and sleeve to attach friction is introduced. Because of how sticky deposits are this friction can become very large which acts as a brake on the needle slowing both opening and closing. This would lead to a delay for both Start Of Injection (SOI) and a delayed EOI. For low friction this would mean the effective time the needle is open is longer and total injection per cycle is therefore larger. For high friction the needle will not be able to lift high enough to provide full fuel flow injection and this will decrease the total injection per cycle.

High friction cases are usually what has been seen in other studies such as Tanaka et al. [22] where they saw a large decrease in needle opening height, delayed SOI and delayed EOI.

When the friction force becomes larger than the opening force the needle cannot open and the injector seizes, leading to engine failure. In a number of cases engines have been reported to have bad performance when running and after have been turned off for several hours they no longer start. This is most probably due to severe friction where, as long as the engine is warm, the tolerances in the injector is slightly larger than when cold and the engine can run. When cold, the tolerances are even smaller and the deposit build-up around the needle is large enough to cause the injector to seize.

6.3 Rig running method

As deposits seem to stick very well to the injector needle and the pressure wave caused by the Joukowski pressure rapidly decrease inside the injector there is probably little to no need to consider deposits tearing from the injector needle and sleeve when running. The limiting factors in the rig will probably be the high pressure fuel pump if component limitations are need to be considered. From Joukowski pressure, discussions and analysis, this project purposes a high fuel injection cycle with opening times similar to having the engine running on maximum torque. Unlike a real engine where the needle is in its closed position about 95% of the time, this project propose to let it be closed 50% of the time, giving a high fuel flow for soft particles the reach the injector, but also a long enough resting time to increase their temperature and attach.

While running the test the flow from the fuel tank should be measured since deposits will affect the needle dynamics and therefore the fuel flow in the injector. Cummins/Scania injectors also have an inbuilt system, AIC, where the common-rail pressure is lowered to take test data and diagnose the injector. It is recommended to use this where the most

considerable changes should be EOI changes. A decrease in EOI is a sign of deposit build-up and can be seen as an earlier pressure spike. Whereas an increase, which probably is much more significant, is a sign of friction where deposits have started to stick together, this can be seen as a delayed pressure spike.

As all components in the testing rig is designed for an eight cylinder engine this test protocol should not be a problem for any of the components. The high pressure pump will run slightly faster than an engine on full power, however this should be within its safety limits. If the pump is overheating it is recommended to increase the closed time of the injector to let the pumps run as they would in a eight cylinder engine on full power. A proposed rig running method can be seen in 6.1.

Table 6.1: Suggestion for a rig running method.

Injector time open:	Set for high fueling
Injector time closed:	Same as Injector time open
Pressure:	Normal common-rail pressure
Temperature:	Between 180 °C-220 °C
Fuel flow data reading:	Every 15 minutes
AIC reading:	Every 5 minutes

7 Conclusion

7.1 Conclusion and Future work

Internal Diesel Injector Deposits are a concern for diesel engine developers with more and more bio diesel mixed into the fuel, causing soft particles. A rig test for development of new injectors is a step towards finding solutions to this problem and to have a reasonable laboratory test in future development. As IDID are sticky and attaches well to injector parts when heated, a heated injector test rig will most probably be able to recreate the issues found in commercial engines.

Running a test rig at high fueling cycles together with short intervals with it being closed gives both a high fuel rate with a lot of soft particles introduced to the system, as well as an adequate resting time where the particles can attach to both injector sleeve and needle. A non-cycle approach where the needle is either fully open or fully closed will most probably result in fuel not being properly heated and soft particles being able to run through the system in the open case and not enough soft particles being introduced to the system for the closed case. It is therefore recommended to have the injector open for a high fuel rate and closed for the same amount of time as its opened interval. This will only be possible in a rig but will decrease the time needed to create changes to the injectors performance.

As for rig testing it is recommended to measure fuel flow and common-rail pressure. The fuel flow will change due to IDID which gives a clue of when they affect the system. The common-rail pressure can say more about how the needle in the injector is affected by IDID by looking at changes in pressure drop and pressure spikes from when the needle is opening respectively closing. These changes are most probably found as delays in time for both pressure drop and pressure spike.

7.2 Future work

For future work it is recommended to first of all get lots of testing done in the test rig to see if the test method works and more important to see what can be done with the rig and injectors to both improve the test method as well as developing new injectors. Another important task could be to do computer simulations of the new forces introduced in the theory section of this report and see how this compares with reality. Since it seems

friction is the main cause for performance changes in the injector it could be an idea to study this in more detail and find a better model for it. This project has presented a suggestion for a test method based on forces and flow inside the fuel injector.

Literature

- [1] H. Jääskeläinen. (2019). 'Early history of the diesel engine', [Online]. Available: https://dieselnet.com/tech/diesel_history.php (accessed March 13, 2020).
- [2] J. Ullmann, M. Geduldig, H. Stutzenberger, R. Caprotti, and G. Balfour, "Investigation into the formation and prevention of internal diesel injector deposits", in *SAE World Congress Exhibition*, SAE International, April 2008.
- [3] S. D. Schwab, J. J. Bennett, S. J. Dell, J. M. Galante-Fox, A. M. Kulinowski, and K. T. Miller, "Internal injector deposits in high-pressure common rail diesel engines", in *SAE 2010 Powertrains Fuels Lubricants Meeting*, SAE International, October 2010.
- [4] S. de Goede, R. Barbour, A. Velaers, B. Sword, D. Burton, and K. Mokheseng, "The effect of near-zero aromatic fuels on internal diesel injector deposit test methods", in *WCX™ 17: SAE World Congress Experience*, SAE International, March 2017.
- [5] M. Alves Fortunato, F. Lenglet, A. Ben Amara, and L. Starck, "Are internal diesel injector deposits (idid) mainly linked to biofuel chemical composition or/and engine operation condition?", in *International Powertrains, Fuels Lubricants Meeting*, SAE International, January 2019.
- [6] P. Lacey, S. Gail, D. Grinstead, C. Daveau, R. Caprotti, R. Dallanegra, and D. Pigeon, "Use of a laboratory scale test to study internal diesel injector deposits", in *SAE 2016 International Powertrains, Fuels Lubricants Meeting*, SAE International, October 2016.
- [7] C. Trobaugh, C. Burbrink, Y. Zha, S. Whitacre, C. Corsi, and N. Blizzard, "Internal diesel injector deposits: Theory and investigations into organic and inorganic based deposits", in *SAE/KSAE 2013 International Powertrains, Fuels Lubricants Meeting*, SAE International, October 2013.
- [8] P. Ashna, "Design of a rig for replicating internal diesel injector deposits", Master's thesis, Linköpings Universitet, Sweden, 2019.
- [9] P. Lacey, S. Gail, J. M. Kientz, G. Benoist, P. Downes, and C. Daveau, "Fuel quality and diesel injector deposits", in *SAE 2012 International Powertrains, Fuels Lubricants Meeting*, SAE International, Sep. 2012.

- [10] P. Lacey, S. Gail, J. M. Kientz, N. Milovanovic, and C. Gris, "Internal fuel injector deposits", in *SAE International Powertrains, Fuels and Lubricants Meeting*, SAE International, August 2011.
- [11] J. Barker, J. Reid, M. Piggott, M. W. Fay, A. Davies, C. Parmenter, N. Weston, C. Snape, D. Scurr, and S. Angel-Smith, "The characterisation of diesel internal injector deposits by focused ion-beam scanning electron microscopy (fib-sem), transmission electron microscopy (tem), atomic force microscopy and raman spectroscopy.", in *JSAE/SAE 2015 International Powertrains, Fuels Lubricants Meeting*, SAE International, Sep. 2015.
- [12] A. Ben Amara, B. Lecointe, N. Jeuland, T. Takahashi, Y. Iida, H. Hashimoto, and J. Bouilly, "Experimental study of the impact of diesel/biodiesel blends oxidation on the fuel injection system", in *SAE 2014 International Powertrain, Fuels Lubricants Meeting*, SAE International, October 2014.
- [13] P. A. Risberg and S. Alfredsson, "The effect of zinc and other metal carboxylates on nozzle fouling", in *SAE 2016 World Congress and Exhibition*, SAE International, April 2016.
- [14] N. J. Rounthwaite, R. Williams, C. McGivery, J. Jiang, F. Giulliani, and B. Britton, "A chemical and morphological study of diesel injector nozzle deposits - insights into their formation and growth mechanisms", in *WCX™ 17: SAE World Congress Experience*, SAE International, March 2017.
- [15] H. Bernemyr, B. Csontos, H. Hittig, and O. Forsberg, "Study of nozzle fouling: Deposit build-up and removal", in *2019 JSAE/SAE Powertrains, Fuels and Lubricants*, SAE International, December 2019.
- [16] L. N. Karebi, "Experimental methods to quantify the filtration efficiency of soft particles in bio fuels", Master's thesis, Aalto University, Finland, 2019.
- [17] Bosch, *Bränsle egenskaper Bosch*, Scania internal document, May 23, 2011.
- [18] M. K. K. Hannu Jääskeläinen, "Common Rail Fuel Injection", *DieselNet*, vol. 05, 2015.
- [19] O. K. V. Pavlenko L. Rosenqvist, *Fluid mechanics compendium, version 9*. Uppsala University, Sweden: Department of Physics and Astronomy, September 2014.
- [20] D. Miller, *Internal flow systems, second edition*. Cranfield, Bedford: BHR Group Limited, 1990.
- [21] R. Alassar, "Hagen-poiseuille flow in tubes of semi-circular cross-sections", in *2011 Fourth International Conference on Modeling, Simulation and Applied Optimization*, April 2011, pp. 1–2.

- [22] A. Tanaka, K. Yamada, T. Omori, S. Bunne, and K. Hosokawa, "Inner diesel injector deposit formation mechanism", in *SAE/KSAE 2013 International Powertrains, Fuels Lubricants Meeting*, SAE International, October 2013.
- [23] A. Bregman. (May 2017). 'Water hammer', [Online]. Available: <https://www.valvemagazine.com/magazine/sections/back-to-basics/8418-water-hammer.html> (accessed March 4, 2020).

Appendices

Script for drag and shear forces due to deposit build-up.

```

1  clear all
2  %R1 = (2:0.001:2.25)*10^-3;
3  %R2 = (3:-0.001:2.75)*10^-3;
4  R1 = (4:0.001:4.25)*10^-3;
5  R2 = (4.5:-0.001:4.25)*10^-3;
6  R1_an = (2:0.001:2.25)*10^-3;
7  R2_an = (3:-0.001:2.75)*10^-3;
8  R = R2-R1;
9  R_diff = 100*R./R(1);
10 m = 0.11;
11 rho = 791.1;
12 Q = m/rho;
13
14 L = 0.0045;
15 L_an = 0.025;
16 tol = 0.000001;
17 mu = 6.175*10^-4; %Ns/m2
18 %mu = linspace(5.1*10^-6,25500,10000);
19 eps = 0.025*10^-3;
20 %rho = 843;
21 alpha = [0,pi/8,pi/4,pi/2];
22
23 for j =1:length(alpha)
24     for i=1:length(R1)
25
26         %flat orifice
27         P(j,i) = 2*pi*R2(i)+2*alpha(j)*R1(i)+2*R1(i)*sin(
                alpha(j));
28         A(j,i) = pi*R2(i)^2-(alpha(j)*R1(i)^2+0.5*R1(i)^2*sin
                (2*alpha(j)));
29         v_fluid(j,i) = Q/A(j,i);
30         v(j,i) = v_fluid(j,i);
31         Dh(j,i) = 4*A(j,i)/P(j,i);
32         S(j,i) = 2*alpha(j)*R1(i)+2*R1(i)*sin(alpha(j));
33         Re(j,i) = m*Dh(j,i)/(mu*A(j,i));
34         fric(j,i) = darcy_friction(Dh(j,i),eps,Re(j,i),tol);
35
36         Ac(j,i) = (2.457*log(((7/Re(j,i))^0.9+0.27*eps/Dh(j,i)
                )^-1))^16;
37         Bc(j,i) = (37530/Re(j,i));
38         fd(j,i) = 8*((8/Re(j,i))^12+(Ac(j,i)+Bc(j,i))^-1.5)
                ^ (1/12);

```

```

39
40 %annulus
41 Dh_an(i) = 2*(R2_an(i)-R1_an(i));
42 A_an(i) = pi*((R2_an(i)^2)-(R1_an(i)^2));
43 v_an(i) = Q/A_an(i);
44 S_an(i) = 2*pi*R1_an(i);
45 Re_an(i) = m*Dh_an(i)/(mu*A_an(i));
46 fric_an(i) = darcy_friction(Dh_an(i),eps,Re_an(i),tol
    );
47
48 Reynold(i) = Reynolds(m,rho,mu,R2_an(i),R1_an(i));
49
50 %forces
51 Fr(j,i) = 8*Q^2*S(j,i)*L/(rho*A(j,i)^2);
52 F_needle(j,i) = 8*v(j,i)^2*S(j,i)*L/(rho);
53 Fr_an(i) = 8*Q^2*S_an(i)*L_an/(rho*pi*(R2_an(i)^2-
    R1_an(i)^2)^2);
54 F_anNeedle(i) = 8*v_an(i)^2*S_an(i)*L_an/(rho);
55 F(j,i) = fric(j,i)*Fr(j,i);
56 F_an(i) = fric_an(i)*Fr_an(i);
57 FFD(i) = fd(i)*Fr(i);
58
59 %flat orifice drag
60 F_dragFlat(j,i) = 0.82*0.5*rho*Q^2*((alpha(j)*R1(i)
    ^2+0.5*R1(i)^2*sin(2*alpha(j)))/A(j,i)^2));
61 %annulus drag
62 F_dragAnnu(i) = 0.82*0.5*rho*Q^2*pi*R1_an(i)^2/(A_an(
    i)^2);
63 %drag force
64 F_drag(j,i) = F_dragFlat(j,i);
65
66 F_tot(j,i) = F(j,i)+F_an(i);
67 F_totNeedle(j,i) = F_needle(j,i)+F_anNeedle(i);
68 end
69 j = j+1;
70 end
71
72 figure(1)
73 plot(R_diff,F_tot)
74 set(gca, 'xdir','reverse')
75 xlabel('Gap width, % of original')
76 ylabel('Shear force, N')
77 title('Shear force from deposit build-up')
78
79 figure(2)
80 plot(R_diff,F_drag)

```

```

81 set(gca, 'xdir','reverse')
82 xlabel('Gap width, % of original')
83 ylabel('Drag force, N')
84 title('Drag force from deposit build-up')
85
86 figure(3)
87 plot(R_diff,F_drag(2,:))
88 set(gca, 'xdir','reverse')
89 xlabel('Gap width, % of original')
90 ylabel('Drag force, N')
91 title('Drag force from deposit build-up')

```


Script for shear force due to increased viscosity.

```

1  clear all
2  %R1 = (2:0.001:2.25)*10^-3;
3  %R2 = (3:-0.001:2.75)*10^-3;
4  R1 = 4.245*10^-3;
5  R2 = 4.255*10^-3;
6  R1_an = 2.245*10^-3;
7  R2_an = 2.755*10^-3;
8  m = 0.11;
9  rho = 843;
10 Q = m/rho;
11
12 L = 0.0045;
13 tol = 0.000001;
14 %mu = 5.1*10^1;
15 mu = linspace(1*10^-3,10^6,1000); %Ns/m2 %25500
16 mu_diff = mu./mu(1);
17 eps = 0.025*10^-3;
18 %rho = 843;
19 alpha = pi/4;
20
21 P = 2*pi*R2+2*alpha*R1+2*R1*sin(alpha);
22 A = pi*R2^2-(alpha*R1^2+0.5*R1^2*sin(2*alpha));
23 Dh = 4*A/P;
24 S = 2*alpha*R1+2*R1*sin(alpha);
25 Fr = 8*Q^2*S*L/(rho*pi*(R2^2-R1^2));
26
27 Dh_an = 2*(R2_an-R1_an);
28 A_an = pi*((R2_an^2)-(R1_an^2));
29 S_an = 2*pi*R1_an;
30 Fr_an = 8*Q^2*S_an*L/(rho*pi*(R2_an^2-R1_an^2));
31
32 for i=1:length(mu)
33
34     Re(i) = Q*Dh/(mu(i)*A);
35     if Re(i)<2000
36         fric(i) = 64/Re(i);
37     else
38         fric(i) = darcy_friction(Dh,eps,Re(i),tol);
39     end
40
41     Ac(i) = (2.457*log(((7/Re(i))^0.9+0.27*eps/Dh)^-1))
42         ^16;
43     Bc(i) = (37530/Re(i));

```

```

43     fd(i) = 8*((8/Re(i))^12+(Ac(i)+Bc(i))^(−1.5))^(1/12);
44
45     %annulus
46     Re_an(i) = Q*Dh_an/(mu(i)*A_an);
47     fric_an(i) = darcy_friction(Dh_an,eps,Re_an(i),tol);
48
49     F(i) = fric(i)*Fr;
50     Ff(i) = fd(i)*Fr;
51     F_an(i) = fric_an(i)*Fr_an;
52
53     F_tot(i) = F(i) + F_an(i);
54
55     end
56
57     plot(mu,F_tot)
58     %set(gca, 'xdir','reverse')
59     xlabel('Dynamic viscosity , Ns/m2')
60     ylabel('Shear force , N')
61     title('Shear force from increased viscosity')

```

Script for finding the Darcy friction factor.

```
1 function [ f ] = darcy_friction(Dh, Roughness, Reynolds,
    Tolerance )
2 %Function for finding the Darcy friction factor. Output
    is the factor as it
3 %is
4
5 test = 1;
6 b=1;
7
8 while test>Tolerance
9     a = -2*log10(Roughness/(3.7*Dh)+2.51*b/(Reynolds));
10    b = a;
11    test = abs((1/b^2-1/a^2)/b^2);
12 end
13 f = 1/(b^2);
14 end
```

Script for finding the Reynolds number in a circular annulus.

```
1 function [RE] = Reynolds(m, rho, mu, R2, R1)
2 Q = m/rho; %m^3/s
3 Dh = 2*(R2-R1); %m
4
5 A = pi*(R2^2-R1^2); %m^2
6
7 RE = (Q*rho*Dh)/(mu*A);
8 end
```

